

## A Feedback Real Time Optimization Strategy using a Novel Steady-state Gradient Estimate and Transient Measurements

Dinesh Krishnamoorthy, Esmaeil Jahanshahi, and Sigurd Skogestad

*Ind. Eng. Chem. Res.*, **Just Accepted Manuscript** • DOI: 10.1021/acs.iecr.8b03137 • Publication Date (Web): 03 Dec 2018

Downloaded from <http://pubs.acs.org> on December 5, 2018

### Just Accepted

“Just Accepted” manuscripts have been peer-reviewed and accepted for publication. They are posted online prior to technical editing, formatting for publication and author proofing. The American Chemical Society provides “Just Accepted” as a service to the research community to expedite the dissemination of scientific material as soon as possible after acceptance. “Just Accepted” manuscripts appear in full in PDF format accompanied by an HTML abstract. “Just Accepted” manuscripts have been fully peer reviewed, but should not be considered the official version of record. They are citable by the Digital Object Identifier (DOI®). “Just Accepted” is an optional service offered to authors. Therefore, the “Just Accepted” Web site may not include all articles that will be published in the journal. After a manuscript is technically edited and formatted, it will be removed from the “Just Accepted” Web site and published as an ASAP article. Note that technical editing may introduce minor changes to the manuscript text and/or graphics which could affect content, and all legal disclaimers and ethical guidelines that apply to the journal pertain. ACS cannot be held responsible for errors or consequences arising from the use of information contained in these “Just Accepted” manuscripts.

# A Feedback Real Time Optimization Strategy using a Novel Steady-state Gradient Estimate and Transient Measurements

Dinesh Krishnamoorthy, Esmaeil Jahanshahi, and Sigurd Skogestad\*

*Department of Chemical Engineering, Norwegian University of Science and Technology  
(NTNU), Trondheim, Norway*

E-mail: skoge@ntnu.no

## Abstract

This paper presents a new feedback real-time optimization (RTO) strategy for steady-state optimality that directly uses transient measurements. The proposed RTO scheme is based on controlling the estimated steady-state gradient of the cost function using feedback. The steady-state gradient is estimated using a novel method based on linearizing a nonlinear dynamic model around the current operating point. The gradient is controlled to zero using standard feedback controllers, for example, a PI-controller. In case of disturbances, the proposed method is able to adjust quickly to the new optimal operation. The advantage of the proposed feedback RTO strategy compared to standard steady-state real-time optimization is that it reaches the optimum much faster and without the need to wait for steady-state to update the model. The advantage compared to dynamic RTO and the closely related economic NMPC, is that the computational cost is much reduced and the tuning is simpler. Finally, it is significantly faster than classical extremum-seeking control and does not require the measurement of the cost function and additional process excitation.

## Introduction

Real-time optimization is traditionally based on rigorous steady-state process models that are used by a numerical optimization solver to compute the optimal inputs and setpoints. The optimization problem needs to be re-solved every time a disturbance occurs. This step is also known as “data reconciliation”. Since steady-state process models are used, it is necessary to wait so the plant has settled to a new steady-state before updating the model parameters and estimating the disturbances. It was noted by Darby et al.<sup>1</sup> that this steady-state wait-time is one of the fundamental limitations of the traditional RTO approach.

In the past two decades or so, there have been developments on several alternatives to the traditional RTO. A good classification and overview of the different RTO schemes is found in Chachuat et al.<sup>2</sup>, François et al.<sup>3</sup> and the references therein. Recently, to address the problem of the steady-state wait-time associated with the traditional steady-state RTO, a hybrid RTO approach was proposed by Krishnamoorthy et al.<sup>4</sup>. Here, the model adaptation is done using a dynamic model and transient measurements, whereas the optimization is performed using a static model. The hybrid RTO approach thus requires solving a numerical optimization problem in order to compute the optimal setpoints. It also requires regular maintenance of both the dynamic model and its static counterpart.

With the recent surge of developments in the so-called *direct input adaptation* methods, where the optimization problem is converted to a feedback control problem,<sup>2,3</sup> we here propose to convert the hybrid RTO strategy proposed by Krishnamoorthy et al.<sup>4</sup> into a feedback steady-state RTO strategy. This is based on the principle that optimal operation can be achieved by controlling the estimated steady-state gradient from the inputs to the cost at a constant setpoint of zero. The proposed method involves a novel non-obvious method for estimating the steady-state gradient by linearizing a nonlinear dynamic model which is updated using transient measurements. To be more specific, the nonlinear dynamic model is used to estimate the states and parameters by means of a dynamic estimation scheme in the same fashion as in the hybrid and dynamic RTO approaches. However, instead of using

1  
2  
3 the updated model in an optimization problem, the state and the parameter estimates are  
4 used to linearize the updated dynamic model from the inputs to the cost. This linearized  
5 dynamic model is then used to obtain the mentioned non-obvious estimate of the steady-  
6 state gradient at the current operating point (Theorem 1). Optimal operation is achieved by  
7 controlling the estimated steady-state gradient to constant setpoint of zero by any feedback  
8 controller.  
9

10  
11 The concept of achieving optimal operation by keeping a particular variable at a constant  
12 setpoint is also the idea behind self-optimizing control, which is another direct input adap-  
13 tation method, see Skogestad<sup>5</sup> and Jäschke et al.<sup>6</sup>. It was also noted by Skogestad<sup>5</sup> that  
14 the ideal self-optimizing variable would be the steady-state gradient from the cost to the  
15 input, which when kept constant at a setpoint of zero, leads to optimal operation (thereby  
16 satisfying the necessary condition for optimality), which complements the idea behind our  
17 proposed method.  
18

19  
20 The concept of estimating and driving the steady-state cost gradients to zero is also the  
21 same used in methods such as extremum seeking control,<sup>7,8</sup> necessary-conditions of optimal-  
22 ity (NCO) tracking controllers,<sup>9</sup> and “hill-climbing” controllers.<sup>10</sup> However, these methods  
23 are model-free and hence requires additional perturbations for accurate gradient estimation.  
24 The main disadvantages of such methods are that they require the cost to be measured  
25 directly and generally give prohibitively slow convergence to the optimum.<sup>11,12</sup>  
26

27  
28 The main contribution of this paper is a novel gradient estimation method (Theorem 1),  
29 which is used in a feedback-based RTO strategy using transient measurements. The proposed  
30 method is demonstrated using a CSTR case study. The proposed method is compared with  
31 the traditional static RTO, dynamic RTO and the newer hybrid RTO approach. It is also  
32 compared with two direct input adaptation methods, namely self-optimizing control and  
33 extremum seeking control.  
34  
35  
36  
37  
38  
39  
40  
41  
42  
43  
44  
45  
46  
47  
48  
49  
50  
51  
52  
53  
54  
55  
56  
57  
58  
59  
60

## Proposed Method

In this section, we present the feedback steady-state RTO strategy. Consider a continuous-time nonlinear process,

$$\dot{\mathbf{x}} = \mathbf{f}(\mathbf{x}(t), \mathbf{u}(t), \mathbf{d}(t)) \quad (1)$$

$$\mathbf{y}(t) = \mathbf{h}(\mathbf{x}(t), \mathbf{u}(t))$$

where  $\mathbf{x} \in \mathbb{R}^{n_x}$ ,  $\mathbf{u} \in \mathbb{R}^{n_u}$  and  $\mathbf{y} \in \mathbb{R}^{n_y}$  are the states, process inputs and process measurements respectively.  $\mathbf{d} \in \mathbb{R}^{n_d}$  is the set of process disturbances.  $\mathbf{f} : \mathbb{R}^{n_x} \times \mathbb{R}^{n_u} \times \mathbb{R}^{n_d} \rightarrow \mathbb{R}^{n_x}$  describes the differential equations and the measurement model is given by  $\mathbf{h} : \mathbb{R}^{n_x} \times \mathbb{R}^{n_u} \rightarrow \mathbb{R}^{n_y}$ .

Let the cost that has to be optimized  $J : \mathbb{R}^{n_x} \times \mathbb{R}^{n_u} \rightarrow \mathbb{R}$  be given by,

$$J(t) = \mathbf{g}(\mathbf{x}(t), \mathbf{u}(t)) \quad (2)$$

Note that the measurement model and the cost function are not directly affected by the disturbances but are affected via the states. According to the plantwide control procedure,<sup>5</sup> we also assume that any active constraints are tightly regulated and the  $n_u$  degrees of freedom considered here are the remaining unconstrained degrees of freedom available for optimization.

**Assumption 1.** (2) is sufficiently continuous and twice differentiable such that for any  $\mathbf{d}$ , (2) has a minimum at  $\mathbf{u} = \mathbf{u}^*$ . According to the Karush-Kuhn- Tucker (KKT) conditions, the following then holds:

$$\frac{\partial J}{\partial \mathbf{u}}(\mathbf{u}^*, \mathbf{d}) = \mathbf{J}_{\mathbf{u}}(\mathbf{u}^*, \mathbf{d}) = 0 \quad (3)$$

$$\frac{\partial^2 J}{\partial \mathbf{u}^2}(\mathbf{u}^*, \mathbf{d}) = \mathbf{J}_{\mathbf{uu}}(\mathbf{u}^*, \mathbf{d}) \geq 0 \quad (4)$$

Without loss of generality, we can assume that the optimization problem is a minimization

1  
2  
3 problem.

4  
5 The optimization problem can be converted to a feedback control problem by controlling  
6 the steady-state gradient  $\mathbf{J}_{\mathbf{u}}$  to a constant setpoint of  $\mathbf{J}_{\mathbf{u}}^{sp} = 0$ . The main challenge is  
7 then to estimate the steady-state gradient efficiently. There are many different data-based  
8 gradient estimation algorithms that estimate the steady-state gradient using steady-state  
9 measurements, see Srinivasan et al.<sup>13</sup>. In this paper, we propose to estimate the steady-state  
10 gradient using a nonlinear dynamic model and the process measurements  $y_{meas}$  by means of  
11 a combined state and parameter estimation framework. In this way, we can estimate the  
12 exact gradients around the current operating point.  
13  
14  
15  
16  
17  
18  
19  
20

21 Any state estimation scheme may be used to estimate the states  $\hat{\mathbf{x}}$  and the unmeasured  
22 disturbances  $\hat{\mathbf{d}}$  using the dynamic model of the plant and the measurements  $\mathbf{y}_{meas}$ . In this  
23 paper, for the sake of demonstration, we use an augmented extended Kalman filter (EKF)  
24 for combined state and parameter estimation, see Simon<sup>14</sup> for detailed description of the  
25 extended Kalman filter.  
26  
27  
28  
29  
30

31 Once the states and unmeasured disturbances are estimated, (2) is linearized to obtain  
32 a *local linear dynamic model* from the inputs  $\mathbf{u}$  to the objective function  $J$ . Let  $\tilde{\mathbf{x}}(t)$ ,  $\tilde{\mathbf{u}}(t)$   
33 and  $\tilde{\mathbf{d}}(t)$  denote the original dynamic trajectory that would result if we keep  $\mathbf{u}$  unchanged  
34 (i.e. no control). Let  $\Delta\mathbf{u}(t)$  represent the additional control input and  $\Delta\mathbf{x}(t)$  the resulting  
35 change in the states,  
36  
37  
38  
39  
40  
41  
42

$$\begin{aligned} \mathbf{x}(t) &= \tilde{\mathbf{x}}(t) + \Delta\mathbf{x}(t) \\ \mathbf{u}(t) &= \tilde{\mathbf{u}}(t) + \Delta\mathbf{u}(t) \\ \mathbf{d}(t) &= \tilde{\mathbf{d}}(t) + \Delta\mathbf{d}(t) \end{aligned} \quad (5)$$

43  
44  
45  
46  
47  
48  
49  
50 where we assume  $\tilde{\mathbf{u}}(t) = \hat{\mathbf{u}}(t_0)$  (constant) and  $\tilde{\mathbf{d}}(t) = \hat{\mathbf{d}}(t_0)$  (constant) and  $t_0$  denotes the  
51 current time. Note that  $\Delta\mathbf{d}(t) = 0$  because the control input does not affect the disturbances.  
52 For control purposes, the local linear dynamic model from the inputs to the cost in terms of  
53  
54  
55  
56  
57  
58  
59  
60

the deviation variables is then be given by,

$$\begin{aligned}\Delta\dot{\mathbf{x}} &= A\Delta\mathbf{x}(t) + B\Delta\mathbf{u}(t) \\ \Delta J(t) &= C\Delta\mathbf{x}(t) + D\Delta\mathbf{u}(t)\end{aligned}\tag{6}$$

where  $A \in \mathbb{R}^{n_x \times n_x}$ ,  $B \in \mathbb{R}^{n_x \times n_u}$ ,  $C \in \mathbb{R}^{1 \times n_x}$  and  $D \in \mathbb{R}^{1 \times n_u}$ . The system matrices are evaluated around the current estimates  $\hat{\mathbf{x}}$  and  $\hat{\mathbf{d}}$ ,

$$\begin{aligned}A &= \left. \frac{\partial \mathbf{f}(\mathbf{x}, \mathbf{u}, \mathbf{d})}{\partial \mathbf{x}} \right|_{\mathbf{x}=\hat{\mathbf{x}}(t_0), \mathbf{d}=\hat{\mathbf{d}}(t_0)} \\ B &= \left. \frac{\partial \mathbf{f}(\mathbf{x}, \mathbf{u}, \mathbf{d})}{\partial \mathbf{u}} \right|_{\mathbf{x}=\hat{\mathbf{x}}(t_0), \mathbf{d}=\hat{\mathbf{d}}(t_0)} \\ C &= \left. \frac{\partial \mathbf{g}(\mathbf{x}, \mathbf{u})}{\partial \mathbf{x}} \right|_{\mathbf{x}=\hat{\mathbf{x}}(t_0), \mathbf{d}=\hat{\mathbf{d}}(t_0)} \\ D &= \left. \frac{\partial \mathbf{g}(\mathbf{x}, \mathbf{u})}{\partial \mathbf{u}} \right|_{\mathbf{x}=\hat{\mathbf{x}}(t_0), \mathbf{d}=\hat{\mathbf{d}}(t_0)}\end{aligned}$$

Note that, since we do not assume full state feedback, we need some nonlinear observer to estimate the states  $\hat{\mathbf{x}}$  in order to evaluate the aforementioned Jacobians. Nonlinear observers may not be required if we have full state feedback information to compute the Jacobians, but this is seldom the case.

**Theorem 1.** *Given a nonlinear dynamic system (1) and (2) and assumption 1 holds, the model from the decision variables  $\mathbf{u}$  to the cost  $J$  can be linearized around the current operating point using any nonlinear observer to get (6) and the corresponding steady state gradient is then*

$$\hat{\mathbf{J}}_{\mathbf{u}} = -CA^{-1}B + D\tag{7}$$

*The process can be driven to its optimum by controlling the estimated steady-state gradient to constant setpoint of zero using any feedback control law  $\mathbf{u} = \mathcal{K}(\hat{\mathbf{J}}_{\mathbf{u}})$ .*

**Proof.** In (6),  $\Delta\mathbf{x}(t)$ ,  $\Delta\mathbf{u}(t)$  and  $\Delta J(t)$  are deviation variables. Let  $\Delta\mathbf{u}(t) = \delta\mathbf{u}$  be a small step change in the input occurring at  $t = 0$ , which will result in a steady-state change for the system as  $t \rightarrow \infty$ . This will occur when  $\Delta\dot{\mathbf{x}} = 0$  and by eliminating  $\Delta\mathbf{x}(t)$  it follows from (6) that the steady-state change in the cost is

$$\delta J = \lim_{t \rightarrow \infty} \Delta J(t) = (-CA^{-1}B + D) \delta\mathbf{u} \quad (8)$$

Here, the steady-state gradient is defined as  $\mathbf{J}_{\mathbf{u}} = \frac{\delta J}{\delta\mathbf{u}}$  and (7) follows. Driving the estimated steady-state gradients to a constant setpoint of zero ensures satisfying the necessary condition of optimality.

The proposed method is schematically represented in Fig.1. It can be seen that steady-state gradient is obtained from the dynamic model and not from the steady-state model as would be the conventional approach. With a dynamic model we are able to use the transient measurements to estimate the steady-state gradient.

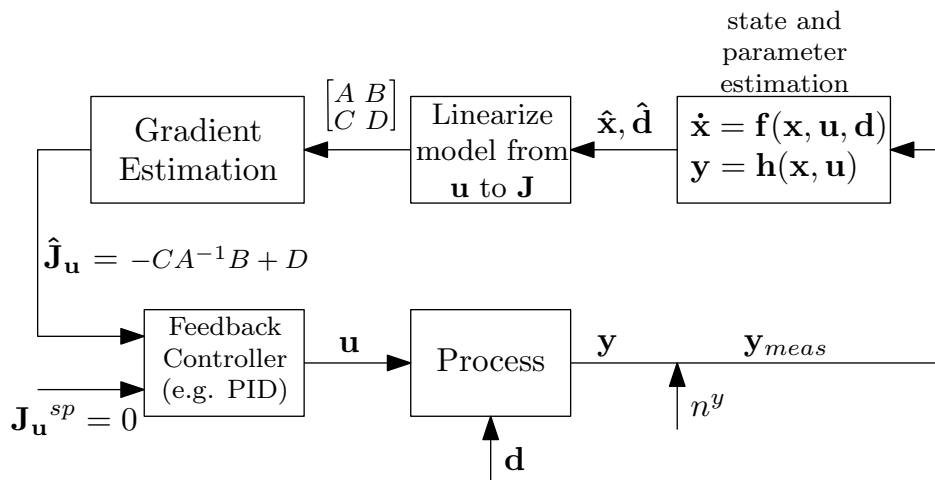


Figure 1: Block diagram of the proposed method

Note that we have used the dynamic model from  $\mathbf{u}$  to  $J$ . To tune the controller, another dynamic model from the inputs  $\mathbf{u}$  to the gradient  $\hat{\mathbf{J}}_{\mathbf{u}}$  is required. The steady-state gain of this model is the Hessian  $\mathbf{J}_{\mathbf{u}\mathbf{u}}$  which is constant if the optimal surface is quadratic and according to Assumption 1 the Hessian does not change sign. In any case, this model is not



the focus of this article. More discussions on controller tuning are provided in the discussions section.

The combined state and parameter estimation framework using extended Kalman filter is discussed in detail by Simon<sup>14</sup>.

Note that, although we use an extended Kalman filter to demonstrate the proposed method in the example, any observer may be used to estimate the states and the parameters. Using the estimated states, the dynamic model may be linearized and the steady state gradient estimated using (6) - (7), which is the key point in the proposed method.

## Illustrative example

In this section, we test the the proposed method using a continuous stirred tank reactor (CSTR) process from Economou et al.<sup>15</sup> (Fig. 2). This case study has been widely used in academic research.<sup>16-18</sup> The proposed method is compared to traditional steady-state RTO, hybrid RTO and dynamic RTO. It also benchmark against two existing direct-adaptation-based method, namely self-optimizing control and extremum seeking control.

## Exothermic Reactor

The CSTR case study consists of a reversible exothermic reaction where component A is converted to component B ( $A \rightleftharpoons B$ ) and the reaction rate is given as  $r = k_1 C_A - k_2 C_B$  where  $k_1 = C_1 e^{\frac{-E_1}{RT}}$  and  $k_2 = C_2 e^{\frac{-E_2}{RT}}$ . The dynamic model consists of two mass balances and an energy balance:

$$\frac{dC_A}{dt} = \frac{1}{\tau}(C_{A,i} - C_A) - r \quad \text{where} \quad \tau = \frac{M}{F} \quad (9a)$$

$$\frac{dC_B}{dt} = \frac{1}{\tau}(C_{B,i} - C_B) + r \quad (9b)$$

$$\frac{dT}{dt} = \frac{1}{\tau}(T_i - T) + \frac{-\Delta H_{rx}}{\rho C_p} r \quad (9c)$$

Here,  $C_A$  and  $C_B$  are concentrations of the two components in the reactor whereas  $C_{A,i}$  and  $C_{B,i}$  are in the inflow.  $T_i$  is the inlet temperature and  $T$  is the reaction temperature. Other model parameters for the process are given in Table 1.

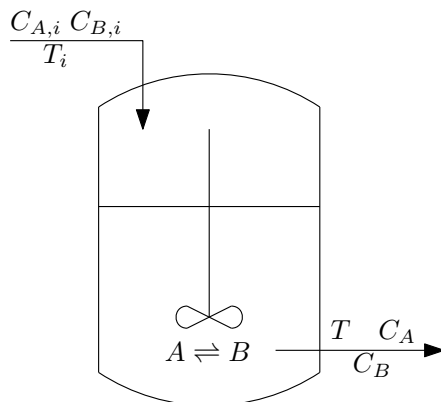


Figure 2: Case 1: Exothermic reactor process

Table 1: Nominal values for CSTR process

	Description	Value	Unit
$F^*$	Feed rate	1	$mol\ min^{-1}$
$C_1$	Constant	5000	$s^{-1}$
$C_2$	Constant	$10^6$	$s^{-1}$
$C_p$	Heat capacity	1000	$cal\ kg^{-1}\ K^{-1}$
$E_1$	Activation energy	$10^4$	$cal\ mol^{-1}$
$E_2$	Activation energy	15000	$cal\ mol^{-1}$
$C_{A,i}^*$	Inlet A concentration	1	$mol\ L^{-1}$
$C_{B,i}^*$	Inlet B concentration	0	$mol\ L^{-1}$
$R$	Universal Gas Constant	1.987	$cal\ mol^{-1}\ K^{-1}$
$\Delta H_{rx}$	Heat of reaction	-5000	$cal\ mol^{-1}$
$\rho$	Density	1	$kg\ L^{-1}$
$\tau$	Time constant	1	$min$

The cost function to be minimize is defined as<sup>16</sup>

$$J = -[2.009C_B - (1.657 \times 10^{-3}T_i)^2]. \quad (10)$$

The manipulated variable is  $u = T_i$ , the temperature in the inlet stream. The state variables are the concentrations and reactor temperature  $x^T = [C_A\ C_B\ T]$ , the disturbances are

1  
2  
3 assumed to be the feed concentrations  $d^T = [C_{A,i} \ C_{B,i}]$ , and the available measurements are  
4  
5  $y^T = [C_A \ C_B \ T \ T_i]$ .  
6  
7

## 8 **Feedback steady-state RTO**

9  
10  
11 The proposed feedback RTO strategy described in section 2 is now implemented for the  
12  
13 CSTR case study. For the state estimation, we use an extended Kalman filter as described  
14  
15 by Simon<sup>14</sup>. The disturbances  $d^T = [C_{A,i} \ C_{B,i}]$  are assumed to be unmeasured and are  
16  
17 estimated together with the states in the extended Kalman filter. A simple PI controller is  
18  
19 used to control the estimated steady-state gradient to a constant setpoint of  $\mathbf{J}_u^{sp} = 0$ . The PI  
20  
21 controller gains are tuned using SIMC tuning rules with the proportional gain  $K_p = 4317.6$   
22  
23 and integral time  $T_I = 60$ s. The process is simulated with a total simulation time of 2400s  
24  
25 with disturbances in  $C_{A,i}$  from  $1 \text{ molL}^{-1}$  to  $2 \text{ molL}^{-1}$  at time  $t = 400$ s and  $C_{B,i}$  from  $0$   
26  
27  $\text{molL}^{-1}$  to  $2 \text{ molL}^{-1}$  at time  $t = 1409$ s. The measurements are assumed to be available with  
28  
29 a sampling rate of 1s.  
30  
31

## 32 **Optimization-based approaches**

33  
34  
35 In this subsection, the simulation results of the proposed method are compared with other  
36  
37 optimization-based approaches, namely traditional static RTO (SRTO), dynamic RTO (DRTO)  
38  
39 and hybrid RTO (HRTO) for the same disturbances as mentioned above. The traditional  
40  
41 static RTO, dynamic RTO and the hybrid RTO structures were used to compute the opti-  
42  
43 mal input temperature computed. Note that, in practice, this could correspond to a setpoint  
44  
45 under the assumption of tight control at the lower regulatory control level.  
46  
47

48  
49 **Traditional static RTO (SRTO)** In this approach, before we can estimate the distur-  
50  
51 bances and update the model, we need to ensure that the system is operating in steady-state.  
52  
53 This is done using a steady-state detection (SSD) algorithm that is commonly used in in-  
54  
55 dustrial RTO system.<sup>19</sup> The resulting steady-state wait time is a fundamental limitation in  
56  
57  
58  
59  
60

many processes and the plant may be operated sub-optimally for significant periods of time before the model can be updated and the new optimal operation re-computed.

**Hybrid RTO (HRTO)** As mentioned earlier, in order to address the steady-state wait time issue of traditional RTO approach, a hybrid RTO approach was proposed,<sup>4</sup> where a dynamic nonlinear model is used online to estimate the parameters and disturbances. The updated static model is then used by a static optimizer to compute the optimal inlet temperature as shown in Fig.3. In this case study, we use the same extended Kalman filter as the one used in the proposed feedback RTO method for the dynamic model adaptation. We then compare the performance of the proposed feedback RTO to the hybrid RTO approach. These two approaches only differ in the fact that in hybrid RTO, a static optimization problem is solved to compute the optimal inlet temperature, whereas in the proposed method optimization is done via feedback.

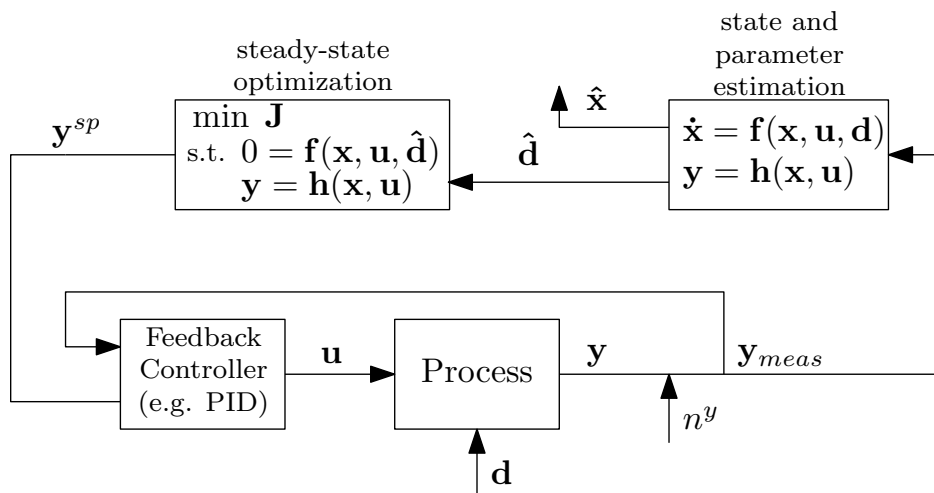


Figure 3: Block diagram of the Hybrid RTO scheme proposed by Krishnamoorthy et al.<sup>4</sup>.

**Dynamic RTO (DRTO)** Recently there has been a surge of research activity towards dynamic optimization and centralized integrated optimization and control such as economic nonlinear model predictive control (EMPC), which is also closely related to dynamic RTO. Since the proposed method uses a nonlinear dynamic model online, a natural question that

1  
2  
3 may arise is why not use the same dynamic models also for optimization. For the sake of  
4 completeness, we therefore compare the performance of the proposed method with dynamic  
5 RTO.  
6  
7  
8

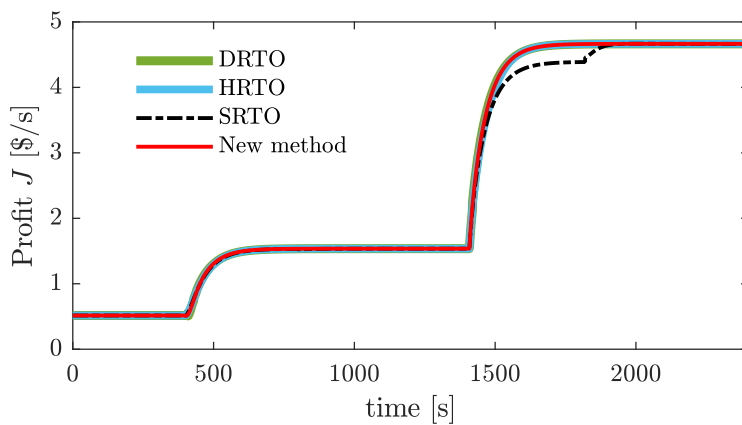
9 For the dynamic RTO, the same extended Kalman filter as in the proposed feedback RTO  
10 method and hybrid RTO was used to update the dynamic model online. The updated non-  
11 linear dynamic model was then used in the dynamic optimization problem with a prediction  
12 horizon of 20 min and a sampling time of 10s.  
13  
14  
15  
16  
17

### 18 **Comparison of RTO methods**

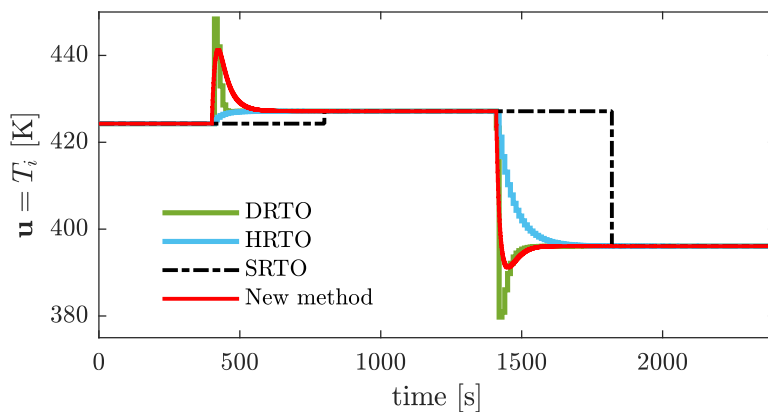
19  
20  
21 The cost  $J$  and the optimal control input  $\mathbf{u}$  provided by the proposed feedback RTO method,  
22 static RTO, hybrid RTO and dynamic RTO are shown in Fig.4a and Fig.4b, respectively.  
23  
24

25 It can be clearly seen that for the static RTO (black dash-dotted lines), the steady-state  
26 wait time delays the model adaptation and hence the system operates sub optimally for  
27 significant time periods. Once the process reaches steady-state and the model is updated,  
28 we see that the steady-state RTO brings the system to the ideal optimal operation. For  
29 example, in this simulation case, it takes around 400s after each disturbances for the SRTO  
30 to update the optimal operating point. The change in the cost observed during the transients,  
31 before the new optimum point is re-computed, is due to the natural drift in the system. This  
32 is more clearly seen after the second disturbance at time  $t = 1400\text{s}$ .  
33  
34  
35  
36  
37  
38  
39  
40

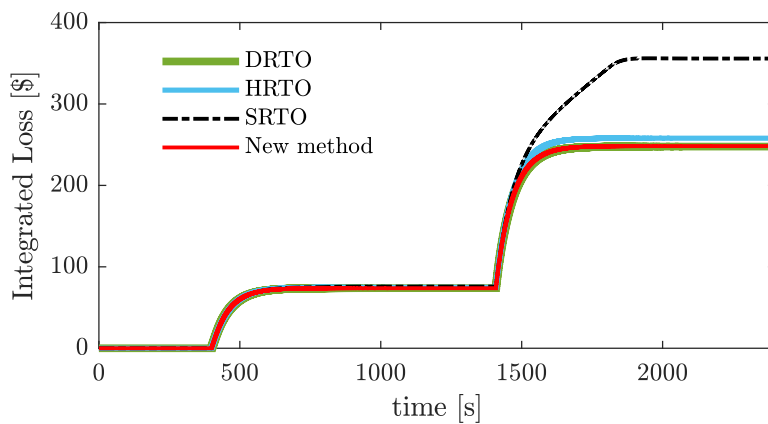
41 Hybrid RTO (cyan solid lines) and dynamic RTO (green solid lines) provide similar  
42 performance as the new proposed feedback RTO strategy (red solid lines), due to the fact that  
43 all these three approaches use transient measurements and a nonlinear dynamic model online.  
44 These three methods however differ in the way the optimization is performed. As mentioned  
45 earlier, dynamic RTO solves a dynamic optimization problem using the updated nonlinear  
46 dynamic model, hybrid RTO solves a static optimization problem using the updated static  
47 counterpart of the model, whereas feedback RTO estimates the steady state gradient by  
48 linearizing the nonlinear dynamic model and controls the estimated steady-state gradients  
49  
50  
51  
52  
53  
54  
55  
56  
57  
58  
59  
60



(a)



(b)



(c)

Figure 4: Simulation results of the proposed feedback RTO method (red solid lines) compared to traditional static RTO (black dash-dotted lines), hybrid RTO (cyan solid lines) and dynamic RTO (green solid lines) for disturbance in  $C_{A,i}$  at time  $t = 400\text{s}$  and  $C_{B,i}$  at time  $t = 1400\text{s}$ . (a) Plot comparing the cost function. (b) Plot comparing the input usage. (c) Plot comparing the integrated loss.

1  
2  
3 to a constant setpoint of zero.  
4

5 The integrated loss is given by  
6

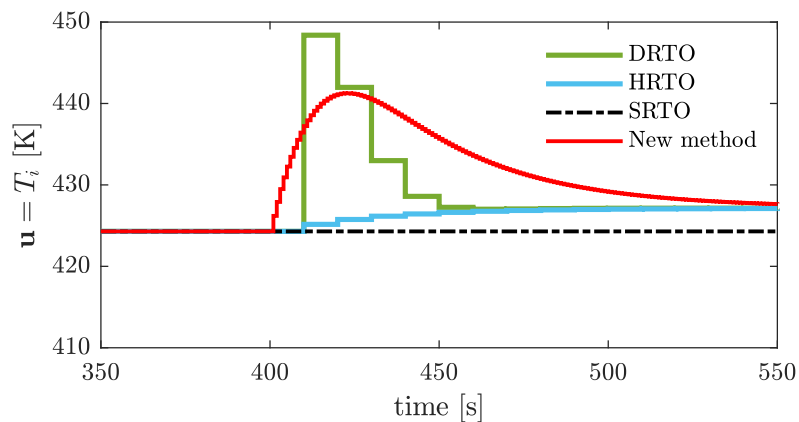
$$L_{int}(t) = \int_0^t (J_{opt,SS}(t) - J(t)) dt. \quad (11)$$

7  
8  
9  
10  
11

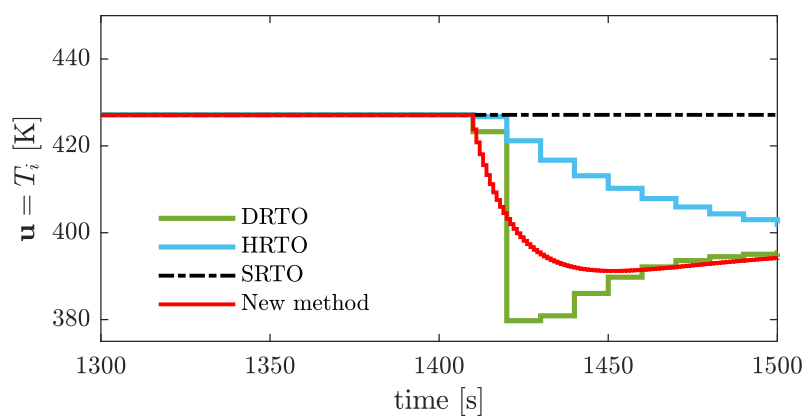
12 To compare the different approaches further, the integrated loss for the different RTO ap-  
13 proaches are shown in Fig.4c and also noted in Table.2 for  $t = 2400s$ .  
14  
15

16 We note here that until time  $t = 1400s$ , the new feedback RTO method has the lowest  
17 loss of 73.73\$ closely followed by DRTO and hybrid RTO with a loss of 73.81\$ and 74.77\$,  
18 respectively. Following the second disturbance, the integrated loss for the interval  $t = 1400s$   
19 to  $t = 2400s$  is the lowest for the DRTO with 247.69\$. The new feedback RTO has a very  
20 similar loss of 248.07\$ followed by hybrid RTO with an integrated loss of 257.97\$. The  
21 static RTO is much worse with a loss of 355.78\$. This is mainly because of the fact that  
22 in the new feedback RTO approach, optimization is done via feedback and hence can be  
23 implemented at higher sampling rate. The static, dynamic and hybrid RTO approaches  
24 requires additional computation time to solve the optimization problem online, and hence  
25 may be implemented at slower sampling rates. As mentioned earlier, in our case study, the  
26 feedback RTO approach is implemented every 1s as opposed to static, dynamic and hybrid  
27 RTO approaches which are solved every 10s. This is clearly shown in Fig.5a, where the  
28 control input from Fig.4b is magnified between time 350s to 550s. Following the disturbance  
29 at  $t = 400s$ , the static, dynamic and hybrid RTO updates the setpoint at time step  $t = 410s$   
30 unlike the feedback RTO, which updates the new control input already at time  $t = 401s$   
31 giving it an advantage over other RTO methods. As a result, the new feedback RTO method  
32 has the lowest integrated loss up to time  $t = 1400s$ . The control input between time 1300s  
33 to 1500s is shown in Fig.5b, where following the disturbance at  $t = 1409s$ , new proposed  
34 feedback RTO, the static, dynamic and hybrid RTO, all update the optimal control input  
35 at time step  $t = 1410s$  simultaneously. Therefore the DRTO has the best integrated loss as  
36  
37  
38  
39  
40  
41  
42  
43  
44  
45  
46  
47  
48  
49  
50  
51  
52  
53  
54  
55  
56  
57  
58  
59  
60

1  
2  
3 expected. This example clearly shows the importance of being able to implement a controller  
4  
5 at higher sampling rates.  
6  
7



(a)



(b)

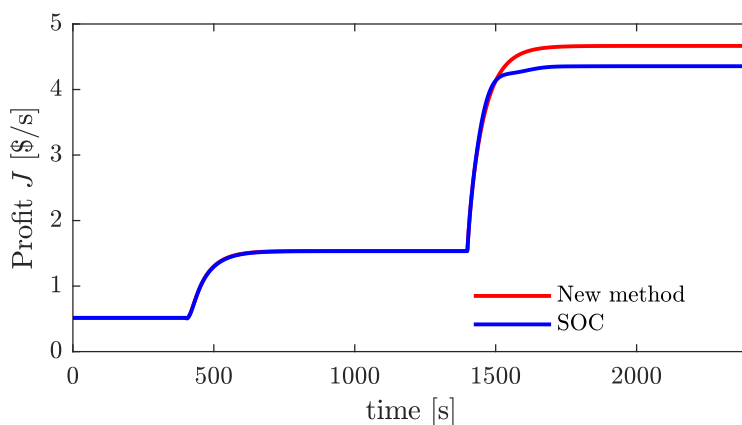
39 Figure 5: Magnified plot of the control input from Fig.4b between time (a) 350s to 550s and  
40 (b) 1300s to 1500s.  
41  
42

43 The simulations are performed on a workstation with the Intel Core i7-6600U CPU (dual-  
44 core with the base clock of 2.60GHz and turbo-boost of 3.40GHz ), and 16GB memory. The  
45 average computation times for the different RTO approaches are also compared in Table 2.  
46 The proposed feedback RTO method is the least computationally intensive method due to  
47 the fact the optimization is done via feedback, and as expected, dynamic RTO is the most  
48 computationally intensive.  
49  
50  
51  
52  
53  
54  
55  
56  
57  
58  
59  
60

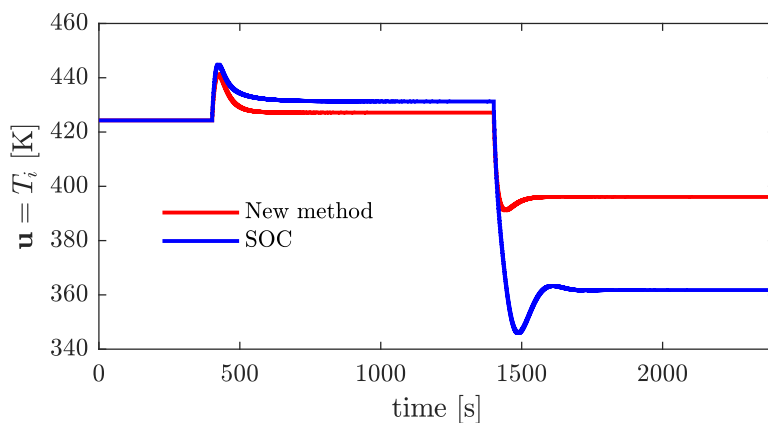


Table 2: Average computation time and integrated loss at the end of simulation time for the proposed method compared with traditional static RTO, hybrid RTO and economic MPC.

	Computation time [s]	Integrated loss $t = 1400s$ [\$]	Integrated loss $t = 2400s$ [\$]
New method	0.004	73.73	248.07
SRTO	0.007	75.75	355.78
HRTO	0.01	74.77	257.97
DRTO	0.14	73.81	247.69



(a)



(b)

Figure 6: Simulation results of the proposed feedback RTO method (red solid lines) compared to self-optimizing control (blue solid lines) for disturbance in  $C_{A,i}$  at time  $t = 400s$  and  $C_{B,i}$  at time  $t = 1400s$ . (a) Plot comparing the cost function. (b) Plot comparing the input usage.

## Comparison with direct-input adaptation methods

In this subsection, we compare the proposed method with two direct input adaptation based methods, namely, self-optimizing control and extremum seeking control.

**Self-optimizing control (SOC)** Since we have 3 measurements, 2 disturbances and 1 control input, the nullspace method can be used to identify the self-optimizing variable. For the case-study considered here, the optimal selection matrix computed using nullspace method (around the nominal optimal point when  $d^T = [C_{A,i} \ C_{B,i}] = [1.0 \ 0.0]$ ) is given by  $\mathbf{H} = \begin{bmatrix} -0.7688 & 0.6394 & 0.0046 \end{bmatrix}$ , see Alstad<sup>16</sup>, Ch.4. The resulting self-optimizing variable  $\mathbf{c} = -0.7688C_A + 0.6394C_B + 0.0046T$  is controlled to a constant setpoint of  $\mathbf{c}_s = 1.9012$ . The PI controller tunings used in the self-optimizing control structure were tuned using SIMC rules with proportional gain  $K_p = 188.65$  and integral time  $T_I = 75\text{s}$ .

The simulations were performed with the same disturbances as in the previous case. The objective function for the two methods are shown in Fig.6a and the corresponding control input usage is shown in Fig.6b. When compared to self-optimizing control, we can see that there is an optimality gap when the disturbances occur. This is because self-optimizing control is based on linearization around the nominal optimal point, as opposed to linearization around the current operating point in the proposed feedback RTO approach. Because of the nonlinear nature of the processes, the economic performance degrades for operating points far from the nominal optimal point hence leading to steady-state losses.

**Extremum seeking control (ESC)** The concept of estimating and driving the steady-state gradient to zero in the proposed feedback RTO strategy is also used in data-driven methods such as extremum seeking control and NCO-tracking. However, the methods are fundamentally different, and complementary rather than competing.

For the sake of brevity, we restrict our comparison to extremum seeking control. We consider the least-square based extremum seeking control proposed by Hunnekens et al.<sup>20</sup>

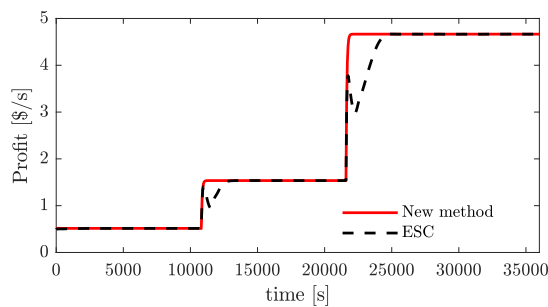
1  
2  
3 because it has been shown to provide better performance than classical extremum seeking  
4 control.<sup>20,21</sup> The least square based extremum seeking controller also estimates the gradi-  
5 ent rather than just the sign of the gradient.<sup>22</sup> The least-square based extremum seeking  
6 controller estimates the steady-state gradient using the measured cost and input data with  
7 the moving window of fixed length in the past. The gradient estimated by the least square  
8 method is then driven to zero using a simple integral action. The integral gain was chosen  
9 to be  $K_{ESC} = 2$ .

10  
11 Due to the slow convergence of the extremum seeking controller, the process with simu-  
12 lated with a total simulation time of 600min with disturbances in  $C_{A,i}$  from  $1 \text{ molL}^{-1}$  to  $2$   
13  $\text{molL}^{-1}$  at time  $t = 10800\text{s}$  and  $C_{B,i}$  from  $0 \text{ molL}^{-1}$  to  $2 \text{ molL}^{-1}$  at time  $t = 21600\text{s}$ . The re-  
14 sults using extremum seeking control are compared with that the of the proposed method in  
15 Fig.7a. It can be seen that the extremum seeking controller reaches the optimal point, how-  
16 ever, the convergence to the optimum point is very slow compared to the proposed method.  
17 The proposed method has a fast action to the disturbances and hence reaches the optimum  
18 significantly faster than the extremum seeking controller. The integrated loss compared to  
19 the ideal steady-state optimum (11) shown in Fig.7c reflects this.

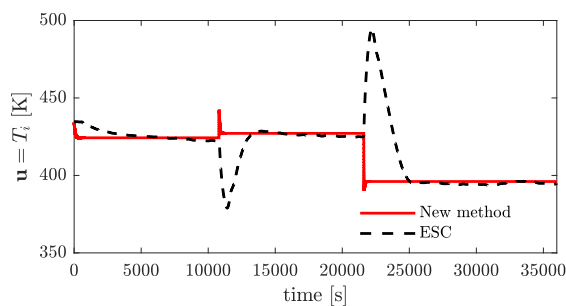
20  
21 It should be added this is a simulation example, because strictly speaking it may not be  
22 possible to directly measure an economic cost  $J$  with several terms. The simple cost in (10)  
23 may be computed by measuring individually the composition  $C_B$  and the inlet temperature  
24  $T_i$ , but more generally for process systems, direct measurement of all the terms and adding  
25 them together is not accurate. This is discussed further in the discussions section.

## 26 27 28 29 30 31 32 33 34 35 36 37 38 39 40 41 42 43 44 45 46 47 **Other multivariable case studies**

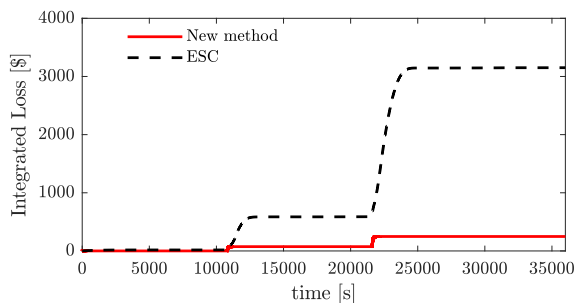
48  
49 In addition to the CSTR case study, the new proposed feedback RTO method has been  
50 successfully applied to a 3-bed ammonia reactor case study by Bonnowitz et al.<sup>23</sup> and to an  
51 oil and gas production optimization problem by Krishnamoorthy et al.<sup>24</sup>. In all these case  
52 studies, the new feedback RTO method was compared with other optimization methods and  
53  
54  
55  
56  
57  
58  
59  
60



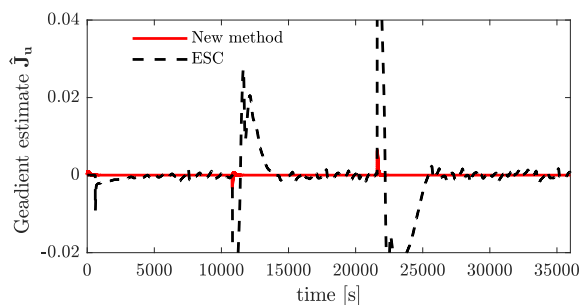
(a)



(b)



(c)



(d)

Figure 7: Comparison of the proposed feedback RTO method (red solid lines) with extremum seeking control (black dashed lines) for disturbance in  $C_{A,i}$  at time  $t = 10800s$  and  $C_{B,i}$  at time  $t = 21600s$ . (a) Plot comparing the cost function. (b) Plot comparing the input usage. (c) Plot comparing the integrated loss. (d) Plot comparing the estimated gradients.

1  
2  
3 was shown to provide consistent results as in the CSTR case study shown in this paper. It is  
4 worth noting that both these cases studies are multivariable processes, where the steady-state  
5 gradients must be estimated and controlled to zero.  
6  
7

8  
9 For example, let's consider the ammonia reactor process studied by Bonnowitz et al.<sup>23</sup>,  
10 which consists of 3 ammonia reactor beds. The optimization problem is concerned with  
11 computing the three optimal feeds in order to maximize the reaction extent. The proposed  
12 method was applied to this system, where the steady-state gradients of the cost with respect  
13 to the three inputs were estimated using (7). The reader is referred to Bonnowitz et al.<sup>23</sup> for  
14 more detailed information about the process and the simulation results, which shows that  
15 the proposed method works also for multi-input processes that are coupled together.  
16  
17  
18  
19  
20  
21  
22  
23  
24

## 25 Discussion

### 26 Comparison with optimization-based approaches

27  
28  
29 With the traditional steady-state RTO approach, it was seen clearly that the steady-state  
30 wait time resulted in suboptimal operation, clearly motivating the need for alternative RTO  
31 strategies that can use transient measurements. Dynamic optimization frameworks, such as  
32 DRTO and economic MPC that use transient measurements, provide the optimal solution,  
33 but it comes at the cost of solving computationally intensive optimization problems as noted  
34 in Table.2. This is even worse for large-scale systems where the sample time will be restricted  
35 by the computational time. Indeed, the computational delay has also been shown to result  
36 in performance degradation or even instability.<sup>25</sup>  
37  
38  
39  
40  
41  
42  
43  
44  
45  
46

47  
48 The feedback RTO strategy proposed in this paper is closely related to the recently  
49 proposed hybrid RTO scheme<sup>4</sup> and has similar performance (see Fig.4a). The main difference  
50 is that in the new strategy, the steady-state gradient is obtained as part of the solution to  
51 the estimation problem and the optimization is then solved by feedback control rather than  
52 numerically solving a steady-state optimization problem. Thus we avoid maintaining the  
53  
54  
55  
56  
57  
58  
59  
60

1  
2  
3 steady-state models in addition to the dynamic model.( i.e. avoids duplication of models  
4 and it avoids the numerical optimization).

5  
6  
7 However, a drawback of the proposed method is that it cannot handle changes in the  
8 active constraint set as easily as optimization-based methods. Changes in active constraint  
9 set would require redesign and re-tuning of the feedback controllers.  
10  
11  
12

## 13 14 15 **Comparison with self-optimizing control**

16  
17 Self-optimizing control is based on linearization around the nominal optimal point. The  
18 economic performance degrades for operating points far from the nominal optimal point due  
19 to the nonlinear nature of the process. This is reason for the sustained steady-state loss of  
20 self-optimizing control seen in the simulation results. The proposed method however, is based  
21 on linearization around the current operating point and hence does not lead to steady-state  
22 losses. The price for this performance improvement is the use of the model online instead of  
23 offline. In other words ,the proposed method requires computational power for the nonlinear  
24 observers which are not required in the standard self-optimizing control. However, nonlinear  
25 observers such as extended Kalman filters can be used, as demonstrated in the simulations,  
26 which are known to be simple to implement and computationally fast.<sup>26</sup> The EKF used in  
27 the simulations had an average computation time of 0.0036s.  
28  
29  
30  
31  
32  
33  
34  
35  
36  
37  
38  
39  
40

## 41 42 **Comparison with extremum seeking control**

43  
44 As mentioned earlier, extremum seeking control estimates the steady-state gradient by fitting  
45 a local linear static model using the cost measurements. Therefore, transient measurements  
46 cannot be used for the gradient estimation. On the other hand, since our proposed method  
47 linearizes the nonlinear dynamic system to get a local linear *dynamic* model, it does not  
48 require a timescale separation for the gradient estimation. Hence the convergence to the  
49 optimum is significantly faster compared to the extremum seeking control, as demonstrated  
50 in our simulation results.  
51  
52  
53  
54  
55  
56  
57  
58  
59  
60

1  
2  
3 In order to address the issue of time-scale separation in extremum seeking control, Mc-  
4 Farlane and Bacon<sup>27</sup> also considered using a local linear dynamic model to estimate the  
5 steady-state gradient. They proposed to identify a linear dynamic model directly from the  
6 measurements, as opposed to estimating the states using a nonlinear dynamic model as in  
7 our proposed method. Therefore, the method by McFarlane and Bacon<sup>27</sup> is a data-based  
8 approach that requires persistent and sufficient excitation to identify the local linear dy-  
9 namic system. On the other hand, our proposed approach of estimating the states using a  
10 nonlinear dynamic model and linearizing around the state estimates does not require any  
11 additional perturbation (but at the cost of modelling effort).

12  
13 However, it is also important to note that extremum seeking (and NCO-tracking) ap-  
14 proaches can handle structural uncertainty. The proposed method, like any other model-  
15 based method, works well only when the model is structurally correct. We do note that,  
16 in the presence of plant-model mismatch, the proposed method may lead to an optimality  
17 gap, leading to some steady state loss, unlike the model-free approaches, which would per-  
18 form better. Therefore, extremum seeking or NCO-tracking methods (including modifier  
19 adaptation) methods should be considered to handle structural mismatch.

20  
21 However, in practice, extremum seeking methods may not be completely model-free and  
22 may then suffer from structural errors, although it will be different from when using model-  
23 based optimization. The reason is that a direct measurement of the cost  $J$  is often not  
24 possible, especially if  $J$  is an economic cost with many terms, and it may then be necessary  
25 to use model-based methods to estimate one or more terms in the cost  $J$ . Typically the cost  
26 function for a process plant is of the form,

$$J = c_q Q + c_f F - c_{p1} P_1 - c_{p2} P_2 \quad (12)$$

27  
28 where  $Q$ ,  $F$ ,  $P_1$  and  $P_2$  are flows in [kg/s] of utility, feed and products 1 and 2 respectively,  
29 and  $c_q$ ,  $c_f$ ,  $c_{p1}$ ,  $c_{p2}$  are the corresponding prices in [\$/kg]. In many cases, for example in  
30  
31  
32  
33  
34  
35  
36  
37  
38  
39  
40  
41  
42  
43  
44  
45  
46  
47  
48  
49  
50  
51  
52  
53  
54  
55  
56  
57  
58  
59  
60

1  
2  
3 refineries, the operating profit is made by shifting smaller amounts of the feed to the most  
4 valuable product (1 or 2), and very accurate measurements would be needed for the flows  
5 (F, P1, P2) to capture this. In practice, the best way to get accurate flows is to estimate  
6 them using a nonlinear process model, e.g., using data reconciliation. This means that  
7 for optimization of larger process systems, an extremum seeking or NCO tracking controller  
8 will not be truly model free, because a model is needed to get an acceptable measurement  
9 (estimate) of the cost.  
10

11  
12 In addition, one main advantage of the proposed method is that it acts on a fast timescale,  
13 thus reaching the optimal point (or near-optimal point in the case of model mismatch) sig-  
14 nificantly faster than model-free approaches which are known to have very slow convergence.  
15 In such cases, model-free methods like ESC or NCO tracking that act in the slow timescale  
16 can be placed on top of the proposed method to account for the plant-model mismatch (e.g.  
17 Jäschke and Skogestad<sup>17</sup>, Straus et al.<sup>28</sup>).

18  
19 Table 4 summarizes the advantages and disadvantages of the proposed method compared  
20 to other tools commonly used for real-time optimization. With this comparison we want to  
21 stress that our new proposed method is not a replacement of any other method but rather  
22 adds to the toolbox of available methods for economic optimization.  
23  
24  
25  
26  
27  
28

## 29 Tuning

30  
31 As mentioned earlier, the steady-state gradient is controlled to a constant setpoint of zero  
32 using feedback controllers. The controller tuning is briefly discussed in this section. For the  
33 CSTR case study, PI controllers were used. The PI controllers were tuned using the SIMC  
34 PID tuning rules.<sup>29</sup> For each input, let the process model from the corresponding gradient  
35  $\mathbf{y} = \mathbf{J}_u$  to the input  $\mathbf{u}$  be approximated by a first order process. For a scalar case,  
36  
37  
38

$$39 \mathbf{J}_u = \frac{\mathbf{k}}{(\tau_1 s + 1)} e^{-\theta s} \mathbf{u} \quad (13)$$



1  
2  
3 where,  $\tau_1$  is the dominant time constant,  $\theta$  is the effective time delay and  $\mathbf{k}$  is the steady-state gain. These three parameters can be found experimentally or from the dynamic  
4 steady-state gain. These three parameters can be found experimentally or from the dynamic  
5 model.<sup>29</sup> Note that the process dynamics include both the effect of the process itself and  
6 the estimator, see Figure 1. In our case we found experimentally by simulations that  $\mathbf{k} =$   
7  $2.25 \times 10^{-4}$ ,  $\tau_1 = 60\text{s}$ ,  $\theta = 1\text{s}$ . The time delay for the process is very small, and mainly  
8 caused by the sampling time of 1 s.  
9

10  
11 In general, the steady-state gain is equal to the Hessian,  $\mathbf{K} = \mathbf{J}_{\mathbf{uu}}$ , which according to  
12 Assumption 1 should not change sign. The Hessian  $\mathbf{J}_{\mathbf{uu}}$  was computed for the CSTR case  
13 study and it was verified that this assumptions holds. In particular, the value of  $\mathbf{K} = \mathbf{J}_{\mathbf{uu}}$  for  
14 the three steady-states shown in Fig. 4 were  $\mathbf{J}_{\mathbf{uu}} = 2.25 \times 10^{-4}$  (nominal),  $\mathbf{J}_{\mathbf{uu}} = 3.89 \times 10^{-4}$   
15 and  $\mathbf{J}_{\mathbf{uu}} = 6.33 \times 10^{-4}$ , respectively. The gain increases by a factor of 3, which may lead to  
16 instability, but if robust PID tunings are used, tuning the controller at the nominal point  
17 should be sufficient. For a PI-controller,  
18  
19

$$20 \quad c(s) = K_C + \frac{K_I}{s} \quad (14)$$

21  
22 the SIMC-rules give the proportional and integral gain<sup>29</sup>  
23  
24

$$25 \quad K_C = \frac{1}{\mathbf{k}} \frac{\tau_1}{\tau_c + \theta} \quad K_I = \frac{K_C}{T_I} \quad (15)$$

26  
27 where the integral time is  $T_I = \min(\tau_1, 4(\tau_c + \theta))$  and  $\tau_c$  is the desired closed-loop time  
28 response time constant which is the sole tuning parameter.<sup>29</sup>  
29

30  
31 It is generally recommended to select  $\tau_c \geq \theta$ <sup>29</sup> to avoid instability and a larger  $\tau_c$  gives  
32 less aggressive control and more robustness. In our case, the controlled variable is  $\mathbf{J}_{\mathbf{u}}$  (the  
33 gradient), but there is little need to control  $\mathbf{J}_{\mathbf{u}}$  tightly because it is not an important variable  
34 in itself. Therefore, to get better robustness we recommend selecting a larger value for  $\tau_c$   
35  
36  
37  
38  
39  
40  
41  
42  
43  
44  
45  
46  
47  
48  
49  
50  
51  
52  
53  
54  
55  
56  
57  
58  
59  
60

(assuming that  $\tau_1 > \theta$ , which is usually the case):

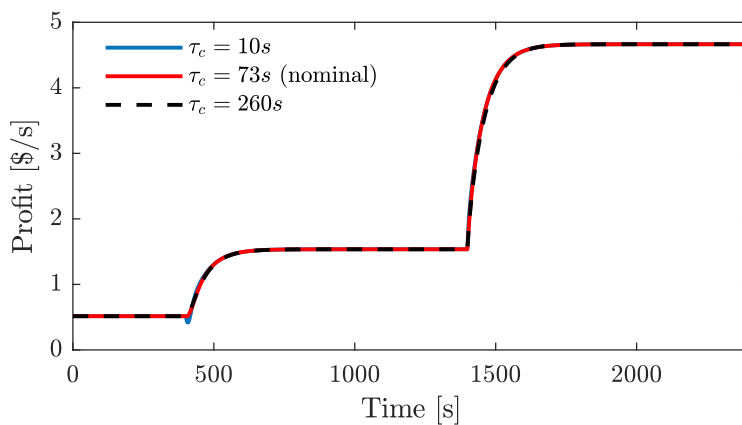
$$\tau_c \geq \tau_1 \quad (16)$$

Selecting  $\tau_c > \tau_1$  means that the closed-loop response is slower than the open-loop response. This avoids excessive use of the input  $\mathbf{u}$  and the system is more robust with respect to gain variations. This is confirmed by the simulations in Fig.8b for three different choices of  $\tau_c$ . With  $\tau_c = 10\text{s} \ll \tau_1 = 60\text{s}$ , we get aggressive input changes with large overshoots in  $\mathbf{u} = T_{in}$  for both disturbances. The control of gradient is good (Fig.8c), but this in itself is not important, and the improvement in profit  $J$  is fairly small compared to the choice  $\tau_c = \tau_1 = 60\text{s}$ , which is the nominal value used previously. The integrated loss when  $\tau_c = 10\text{s}$  was 245.99\$ as opposed to 248.07\$ when  $\tau_c = \tau_1 = 60\text{s}$ . With  $\tau_c = 4\tau_1$  the input change is even smoother, but the performance in terms of the profit ( $J$ ) is almost the same (with an integrated loss of 259.07\$).

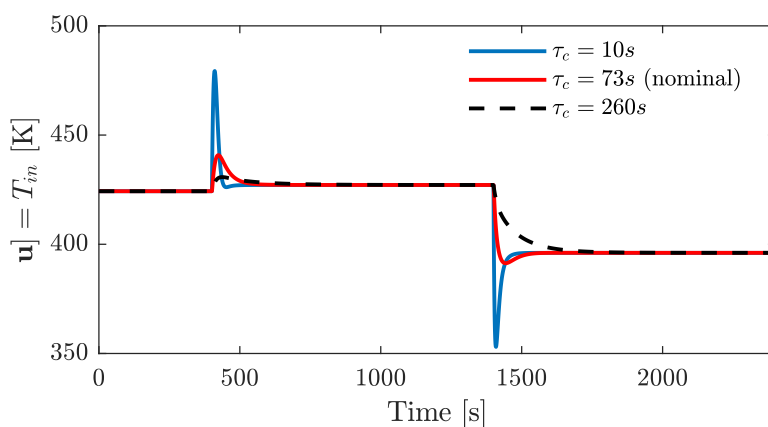
## Stability Robustness

The stability of the system is determined by the closed-loop stability involving the plant input  $\mathbf{u}$  (manipulated variable) and the estimated gradient  $\mathbf{J}_{\mathbf{u}}$  as the plant output  $\mathbf{y}$ . Thus, the overall plant for this analysis includes the real process, the estimator (extended Kalman Filter in our case) and the “measurement”  $\mathbf{y} = \mathbf{J}_{\mathbf{u}} = CA^{-1}B + D$ . In this case we use a simple PI-controller and the conventional linear measures for analyzing robustness are to compute the gain margin, phase margin or delay margin, or H-infinity measures such as the peak of the sensitivity function,  $M_S$ .

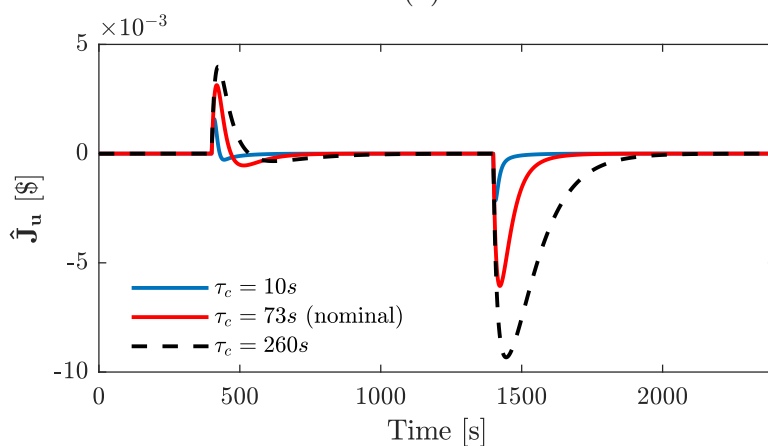
The gain and phase margins at the three different steady-states are shown for the three alternative PI-controllers in Table 3. Note that the gain margin varies from 17.3-6.14 for the least robust controller with  $\tau_c = 10\text{s}$ , which is still much larger than the expected variations in the process gain (which is about a factor 3 from  $2.25 \times 10^{-4}$  to  $6.33 \times 10^{-4}$ ). This is of course



(a)



(b)



(c)

Figure 8: Effect of controller tuning ( $\tau_c$ ) for the new method. (a) Objective function  $J$ . (b) Control input  $\mathbf{u}$ . (c) Estimated gradient  $\hat{\mathbf{J}}_{\mathbf{u}}$ .

a nonlinear plant and the conventional linear analysis of closed-loop stability will have the same limitations as it has for any nonlinear plant. It is also possible to consider nonlinear controllers for the plant, but it does not seem necessary because of the large robustness margins for the linear controllers.

Table 3: Gain and Phase Margins at the different steady-states for the three PI controllers with varying  $\tau_c$ .

		Gain Margin	Phase Margin
Steady-state 1	$\tau_c=10\text{s}$	17.3	84.8°
	$\tau_c=60\text{s}$	95.8	89.1°
	$\tau_c=240\text{s}$	379	89.8°
Steady-state 2	$\tau_c=10\text{s}$	9.99	81.0°
	$\tau_c=60\text{s}$	55.4	88.4°
	$\tau_c=240\text{s}$	219	89.6°
Steady-state 3	$\tau_c=10\text{s}$	6.14	75.3°
	$\tau_c=60\text{s}$	34.1	87.4°
	$\tau_c=240\text{s}$	135	89.3°

In summary, stability is not an important concern for the tuning of the controllers in our case. The important issue is the trade-off between input usage and the speed of response. This was also observed in the other case studies.<sup>23,24</sup>

## Conclusion

To conclude, we propose a novel model-based direct input adaptation approach, where the steady state gradient  $\mathbf{J}_u$  is estimated as  $\hat{\mathbf{J}}_u = -CA^{-1}B + D$  by linearizing the nonlinear model around the current operating point. The nonlinear model and thus the steady-state gradient is updated using transient measurements. It is based on well-known components in the control theory, namely state estimation and simple feedback control. Since a dynamic model is linearized around the current operating point, the method does not need to wait for the process to reach steady-state before updating the next move. The proposed method also does not require additional perturbations for the gradient estimation as opposed to

Table 4: Advantages and disadvantages of the proposed method compared to other RTO approaches

	self-optimizing control <sup>a</sup>	extremum seeking control <sup>b</sup>	new proposed method (Feedback RTO)	Static RTO	Hybrid RTO	economic MPC/Dynamic RTO <sup>c</sup>
Cost Measured	No	Yes	No	No	No	No
Model	static model used offline	Model-free	dynamic model used online	static model used online	static and dynamic model used online	dynamic model used online
perturbation	No	Yes	No	No	No	No
Transient measurements	Yes	No	Yes	No	Yes	Yes
Long-term performance	near-optimal	Optimal <sup>e</sup>	Optimal <sup>d</sup>	Optimal <sup>d,f</sup>	Optimal <sup>d</sup>	Optimal <sup>d</sup>
Convergence time	very fast	very slow	fast	slow <sup>f</sup>	fast	fast <sup>g</sup>
Handle change in active constraints	No	No	No	Yes	Yes	Yes
Numerical solver	No	No	No	static	static	dynamic
Computational cost	very low	very low	low	intermediate	intermediate	high

<sup>a</sup> SOC is complementary to the other methods that should ideally be used in combination.

<sup>b</sup> NCO tracking also has similar properties but can also track changes in active constraints in addition.

<sup>c</sup> Economic MPC typically has non-economic control objectives in addition to the economic objectives in the cost function, whereas DRTO has only economic objectives.

<sup>d</sup> If model is structurally correct.

<sup>e</sup> requires time scale separation between system dynamics, dither and convergence. Sub-optimal operation for long periods following disturbances.

<sup>f</sup> Slow due to steady-state wait time. Sub-optimal operation for long periods following disturbances.

<sup>g</sup> limited by computation time.

1  
2  
3 extremum seeking control. By using the model online, the proposed method can reduce  
4 steady-state losses associated with self-optimizing control. The proposed feedback RTO  
5 method is similar to the recently proposed hybrid RTO (HRTO),<sup>4</sup> but involves a novel way  
6 of estimating the steady-state gradient and instead solves the optimization by feedback. This  
7 is robust and simple and avoids maintaining a steady-state model. The proposed method is  
8 tested in simulations, and compared to commonly used optimization-based approaches and  
9 direct-input adaptation based approaches. The simulation results show that the proposed  
10 method is accurate, fast and easy to implement. The proposed method thus adds on to  
11 the existing tool box of approaches for real-time optimization, and can be useful for certain  
12 cases.  
13  
14  
15  
16  
17  
18  
19  
20  
21  
22  
23  
24

## 25 Acknowledgement

26  
27  
28 The authors gratefully acknowledge the financial support from SFI SUBPRO, which is fi-  
29 nanced by the Research Council of Norway, major industry partners and NTNU.  
30  
31  
32  
33  
34

## 35 References

- 36  
37  
38 (1) Darby, M. L.; Nikolaou, M.; Jones, J.; Nicholson, D. RTO: An overview and assessment  
39 of current practice. *Journal of Process Control* **2011**, *21*, 874–884.  
40  
41  
42 (2) Chachuat, B.; Srinivasan, B.; Bonvin, D. Adaptation strategies for real-time optimiza-  
43 tion. *Computers & Chemical Engineering* **2009**, *33*, 1557–1567.  
44  
45  
46 (3) François, G.; Srinivasan, B.; Bonvin, D. Comparison of six implicit real-time optimiza-  
47 tion schemes. *Journal Européen des Systèmes Automatisés* **2012**, *46*, 291–305.  
48  
49  
50 (4) Krishnamoorthy, D.; Foss, B.; Skogestad, S. Steady-state Real time optimization using  
51 transient measurements. *Computers and Chemical Engineering* **2018**, *115*, 34–45.  
52  
53  
54  
55  
56  
57  
58  
59  
60

- 1  
2  
3 (5) Skogestad, S. Plantwide control: The search for the self-optimizing control structure.  
4 *Journal of process control* **2000**, *10*, 487–507.  
5  
6  
7  
8 (6) Jäschke, J.; Cao, Y.; Kariwala, V. Self-optimizing control—A survey. *Annual Reviews in*  
9 *Control* **2017**, *43*, 199–223.  
10  
11  
12 (7) Krstić, M.; Wang, H.-H. Stability of extremum seeking feedback for general nonlinear  
13 dynamic systems. *Automatica* **2000**, *36*, 595–601.  
14  
15  
16 (8) Ariyur, K. B.; Krstic, M. *Real-time optimization by extremum-seeking control*; John  
17 Wiley & Sons, 2003.  
18  
19  
20 (9) François, G.; Srinivasan, B.; Bonvin, D. Use of measurements for enforcing the neces-  
21 sary conditions of optimality in the presence of constraints and uncertainty. *Journal of*  
22 *Process Control* **2005**, *15*, 701–712.  
23  
24  
25 (10) Kumar, V.; Kaistha, N. Hill-Climbing for Plantwide Control to Economic Optimum.  
26 *Industrial & Engineering Chemistry Research* **2014**, *53*, 16465–16475.  
27  
28  
29 (11) Tan, Y.; Moase, W.; Manzie, C.; Nešić, D.; Mareels, I. Extremum seeking from 1922 to  
30 2010. Control Conference (CCC), 2010 29th Chinese. 2010; pp 14–26.  
31  
32  
33 (12) Trollberg, O.; Jacobsen, E. W. Greedy Extremum Seeking Control with Applications  
34 to Biochemical Processes. *IFAC-PapersOnLine (DYCOPS-CAB)* **2016**, *49*, 109–114.  
35  
36  
37 (13) Srinivasan, B.; François, G.; Bonvin, D. Comparison of gradient estimation methods  
38 for real-time optimization. 21st European Symposium on Computer Aided Process  
39 Engineering-ESCAPE 21. 2011; pp 607–611.  
40  
41  
42 (14) Simon, D. *Optimal State Estimation, Kalman, H-infinity and Nonlinear Approches*;  
43 Wiley-Interscience: Hoboken, New Jersey, 2006.  
44  
45  
46  
47  
48  
49  
50  
51  
52  
53  
54  
55  
56  
57  
58  
59  
60

- 1  
2  
3 (15) Economou, C. G.; Morari, M.; Palsson, B. O. Internal model control: Extension to  
4 nonlinear system. *Industrial & Engineering Chemistry Process Design and Development*  
5 **1986**, *25*, 403–411.  
6  
7  
8  
9  
10 (16) Alstad, V. Studies on Selection of Controlled Variables. PhD Thesis, 2005.  
11  
12  
13 (17) Jäschke, J.; Skogestad, S. NCO tracking and self-optimizing control in the context of  
14 real-time optimization. *Journal of Process Control* **2011**, *21*, 1407–1416.  
15  
16  
17 (18) Ye, L.; Cao, Y.; Li, Y.; Song, Z. Approximating Necessary Conditions of Optimality as  
18 Controlled Variables. *Industrial & Engineering Chemistry Research* **2013**, *52*, 798–808.  
19  
20  
21 (19) Câmara, M. M.; Quelhas, A. D.; Pinto, J. C. Performance Evaluation of Real Industrial  
22 RTO Systems. *Processes* **2016**, *4*, 44.  
23  
24  
25  
26 (20) Hunnekens, B.; Haring, M.; van de Wouw, N.; Nijmeijer, H. A dither-free extremum-  
27 seeking control approach using 1st-order least-squares fits for gradient estimation. IEEE  
28 53rd Annual Conference on Decision and Control (CDC). 2014; pp 2679–2684.  
29  
30  
31  
32 (21) Chioua, M.; Srinivasan, B.; Guay, M.; Perrier, M. Performance Improvement of Ex-  
33 tremum Seeking Control using Recursive Least Square Estimation with Forgetting Fac-  
34 tor. *IFAC-PapersOnLine (DYCOPS-CAB)* **2016**, *49*, 424–429.  
35  
36  
37 (22) Chichka, D. F.; Speyer, J. L.; Park, C. Peak-seeking control with application to forma-  
38 tion flight. Proceedings of the 38th IEEE Conference on Decision and Control. 1999;  
39 pp 2463–2470.  
40  
41  
42 (23) Bonnowitz, H.; Straus, J.; Krishnamoorthy, D.; Jahanshahi, E.; Skogestad, S. Control  
43 of the Steady-State Gradient of an Ammonia Reactor using Transient Measurements.  
44 *Computer-Aided Chemical Engineering* **2018**, *43*, 1111–1116.  
45  
46  
47 (24) Krishnamoorthy, D.; Jahanshahi, E.; Skogestad, S. Gas-lift Optimization by Controlling  
48  
49  
50  
51  
52  
53  
54  
55  
56  
57  
58  
59  
60



- 1  
2  
3 Marginal Gas-Oil Ratio using Transient Measurements. *IFAC-PapersOnLine* **2018**, *51*,  
4 19–24.  
5  
6  
7  
8 (25) Findeisen, R.; Allgöwer, F. Computational delay in nonlinear model predictive control.  
9 *IFAC Proceedings Volumes* **2004**, *37*, 427–432.  
10  
11  
12 (26) Sun, X.; Jin, L.; Xiong, M. Extended Kalman filter for estimation of parameters in  
13 nonlinear state-space models of biochemical networks. *PloS one* **2008**, *3*, e3758.  
14  
15  
16 (27) McFarlane, R.; Bacon, D. Empirical strategies for open-loop on-line optimization. *The*  
17 *Canadian Journal of Chemical Engineering* **1989**, *67*, 665–677.  
18  
19  
20 (28) Straus, J.; Krishnamoorthy, D.; Skogestad, S. Combining self-optimizing control and  
21 extremum seeking control - Applied to ammonia reactor case study. *Journal of Process*  
22 *control* **2017**,  
23  
24  
25 (29) Skogestad, S. Simple analytic rules for model reduction and PID controller tuning.  
26 *Journal of process control* **2003**, *13*, 291–309.  
27  
28  
29  
30  
31  
32  
33  
34  
35  
36  
37  
38  
39  
40  
41  
42  
43  
44  
45  
46  
47  
48  
49  
50  
51  
52  
53  
54  
55  
56  
57  
58  
59  
60

## Graphical TOC Entry

